MISS RACHEL M BURCKHARDT (Orcid ID : 0000-0001-6290-2534)
DR. CHELSEY M VANDRISSE (Orcid ID : 0000-0001-9139-0443)
PROF. JORGE C ESCALANTE-SEMERENA (Orcid ID : 0000-0001-7428-2811)

Article type : Research Article

New AMP-forming acid:CoA ligases from *Streptomyces lividans*, some of which are posttranslationally regulated by reversible lysine acetylation.

Rachel M. Burckhardt*, Chelsey M. VanDrisse*§, Alex C. Tucker†, and Jorge C. Escalante-Semerena*

Department of Microbiology, University of Georgia, Athens, GA

Current addresses:
*These authors contributed equally to this work
§Division of Biology and Biological Engineering, California Institute of Technology, Pasadena CA 91125
†Gingko Bioworks, Boston, MA 02210

Running title: insights into RLA control of CoA ligases in *S. lividans*

*Corresponding author: Department of Microbiology, University of Georgia, 212C Biological Sciences Building, 120 Cedar Street, Athens, GA 30602, USA; Tel: +1 (706)-542-2651, Email: jcescala@uga.edu URL: www.escalab.com

Authors ORCID numbers:

This article has been accepted for publication and undergone full peer review but has not been through the copyediting, typesetting, pagination and proofreading process, which may lead to differences between this version and the Version of Record. Please cite this article as doi: 10.1111/MMI.14414

RMB, 0000-0001-6290-2534
CMVD, 0000-0001-9139-0443
ACT, 0000-0002-9307-7204
JCES, 0000-0001-7428-2811

Summary

In nature, organic acids are a commonly used source of carbon and energy. Many bacteria use AMP-forming acid:CoA ligases to convert organic acids into their corresponding acyl-CoA derivatives, which can then enter metabolism. The soil environment contains a broad diversity of organic acids, so it is not surprising that bacteria such as *Streptomyces lividans* can activate many of the available organic acids. Our group has shown that the activity of many acid:CoA ligases is posttranslationally controlled by acylation of an active-site lysine. In some cases, the modification is reversed by deacylases of different types. We identified eight new acid:CoA ligases in *S. lividans* TK24. Here, we report the range of organic acids that each of these enzymes can activate, and determined that two newly identified CoA ligases were under NAD^+-dependent sirtuin deacylase reversible lysine (de)acetylation control, four were not acetylated by two acetyltransferases used in this work, and two were acetylated but not deacetylated by sirtuin. This work provides insights into the broad organic-acid metabolic capabilities of *S. lividans*, and sheds light into the control of the activities of CoA ligases involved in the activation of organic acids in this bacterium.

Keywords. Reversible lysine acetylation, sirtuin, *Streptomyces*, acetyltransferases, CoA ligases, proteomics, actinobacteria metabolism, organic acid activation

Introduction

Lysine acetylation is a posttranslational modification (PTM) broadly distributed in cells from all domains of life. Acetylation of the epsilon amino group (*N*ε) of lysyl residues can impact the activity or stability of a protein, and its interactions with other proteins or molecules. Importantly, in some cases lysine acetylation is reversed by deacetylases. Regulation of

protein function by reversible lysine acetylation (hereafter RLA) allows cells to react rapidly to changing environmental conditions (VanDrisse & Escalante-Semerena, 2019, Hentchel & Escalante-Semerena, 2015).

The first enzyme reported to be under RLA control was the acetyl-Coenzyme A (AcCoA) synthetase (Acs, EC 6.2.1.1) of *Salmonella enterica enterica* sv Typhimurium LT2 (hereafter *S. enterica*) (Starai *et al.*, 2002). Like other AMP-forming acyl-CoA synthetases (a.k.a. acetate:CoA ligase) (PF00501, IPR000873) (Gulick, 2009), Acs activates acetate to acetyl-CoA (AcCoA) in two steps via an acetyl-AMP (AcAMP) intermediate (Fig. 1) (Starai & Escalante-Semerena, 2004a).

In vitro activity and structural data indicate that in *S. enterica* Acs (*Se*Acs), the side chain of residue K609 is critical for the conversion of acetate to acetyl-AMP (Gulick *et al.*, 2003, Starai & Escalante-Semerena, 2004b). Acetylation of this catalytic lysine abolishes the adenylylation activity of the enzyme, but does not affect the conversion of acetyl-AMP to AcCoA (Starai & Escalante-Semerena, 2004b). RLA controls the activities of acid:CoA ligases in prokaryotes and eukaryotes (Crosby *et al.*, 2012a, Starai & Escalante-Semerena, 2004b, Gardner *et al.*, 2006, Hallows *et al.*, 2006, Nambi *et al.*, 2013, Tucker & Escalante-Semerena, 2013, Burckhardt *et al.*, 2019). Although the presence of the canonical catalytic lysine is necessary, it is not sufficient for RLA control (Crosby & Escalante-Semerena, 2014, Crosby *et al.*, 2012b, Tucker & Escalante-Semerena, 2013). For example, the methylmalonate:CoA ligase MatB enzyme of *Rhodopseudomonas palustris* is not acetylated even though it contains the conserved catalytic lysine within the so-called acetylation motif. Results of structural biochemical and genetic studies showed that a 21-aa region N-terminal to the acetylation motif was necessary for recognition by the acetyltransferase (Crosby *et al.*, 2012b). Notably, in *Streptomyces lividans* acetylation of the catalytic lysine is modulated by the acetylation of a serine residue closely located to the catalytic lysine (VanDrisse & Escalante-Semerena, 2018). The point to keep in mind here is that the catalytic lysine of CoA ligases is not always accessible to acetyltransferases, and that much remains to be learned about GNAT specificity.

RLA involves i) acetyltransferases that transfer the acetyl group from AcCoA to the epsilon amino ($N\varepsilon$) group of specific lysyl residues of a target protein, and ii) deacetylases that remove the modification. Deacetylases could be either NAD^+-dependent or Zn-dependent, acetate-forming enzymes (Hentchel & Escalante-Semerena, 2015) (Fig. 2). NAD^+-dependent protein deacetylation is relevant to the work reported herein.

In *S. enterica*, the protein acetyltransferase (*Se*Pat) acetylates and inactivates Acs (Starai & Escalante-Semerena, 2004b). The *Se*Pat enzyme belongs to the Gcn5-related *N*-acetyltransferase superfamily (GNAT; PF00583, IPR000182), a family of acetyltransferases found in all domains of life (Vetting *et al.*, 2005, Hentchel & Escalante-Semerena, 2015). *S. enterica* contains only one sirtuin, known as CobB (Tsang & Escalante-Semerena, 1998, Starai *et al.*, 2002).

Past work from our group studied the activity and substrates of *Se*Pat homologues in the Gram-positive actinomycete *Streptomyces lividans*. Notably, this bacterium encodes a type II Pat homologue named *Sl*PatA, in which its two domains are reversed relative to the domains of *Se*Pat (Tucker & Escalante-Semerena, 2013) (Fig. S1). Even though *Sl*PatA acetylates the acetoacetyl-CoA synthetase (*Sl*AacS) of this bacterium, it only poorly acetylates *Sl*Acs (Tucker & Escalante-Semerena, 2013). More recent work identified the type-III acetyltransferase *Sl*PatB as the enzyme that acetylates *Sl*Acs (VanDrisse & Escalante-Semerena, 2018). This same work in *S. lividans* also reported the presence of three different deacetylases, two of which were homologous to the NAD^+-dependent deacetylases SIRT5 and SIRT4. The third deacetylase of *S. lividans* was homologous to the Zn-dependent, acetate-forming deacetylases (Fig. 2).

Here, we report the identification and characterization of eight new *S. lividans* acid:CoA ligases and studied their range of substrates. The enzymatic activity of four of the new CoA ligases was modulated by lysine acetylation.

Insights into the need for the posttranslational control of CoA ligases was reported for the acetate:CoA ligase (a.k.a. acetyl-CoA synthetase, Acs) of *Salmonella* enterica. *In vivo* and *in vitro* evidence supported that idea that RLA control of *Se*Acs was needed to maintain energy charge homeostasis (Chan *et al.*, 2011). That is, in the absence of RLA control, *Se*Acs

reduces the energy charge of the cell below growth-sustaining levels due to the depletion of ATP and the buildup of an unphysiologically high level of AMP. Since AMP-forming ligases are involved in many cellular processes, it is of interest to determine which members of this family of enzymes are under RLA control, and what the reason for such a control is.

Our results reported here are only the initial steps taken to identify and initially characterize acid:CoA ligases in *S. lividans.* Subsequent studies will provide insights into the role RLA in *S. lividans* metabolism and physiology.

Results

***Sl*PatA is expressed in a growth-phase dependent manner**. Since there is precedent that type-II acetyltransferases target acetate:CoA ligases and affect growth of bacteria, we sought to probe for differences in growth of the *S. lividans* Δ*patA* strain compared to the *patA*$^+$ strain. *S. lividans* TK24 *patA*$^+$ and Δ*patA* strains were grown aerobically on rich medium (YEME) or minimal medium supplemented with glucose, maltose, β-hydroxybutyrate, glycerol, or *N*-acetylglucosamine. As shown in figure S2, neither the wild-type nor the Δ*patA* strain exhibited a growth defect on any carbon source tested, indicating that the absence of *Sl*PatA function did not perturb the physiology of this bacterium to the point of resulting in observable phenotypical differences between the two strains under the conditions tested. However, we asked whether the protein acetylation patterns of the two strains differed. To address this point, cultures of the *patA*$^+$ and Δ*patA* strains were grown under the above-mentioned conditions. After cell breakage, proteins present in the soluble fraction of the extracts were resolved by SDS-PAGE and probed by western blot for the presence of *Sl*PatA and the presence of acetyllysine (AcK) in resolved proteins. A schematic of the protocol is shown in figure S3. We expected that if *Sl*PatA acetylated *S. lividans* proteins, differences in the protein acetylation profiles would be detectable using anti-AcK (α-AcK) antibodies.

To correlate the presence of *Sl*PatA with changes in protein acetylation profiles, we probed each lysate using rabbit polyclonal antibodies against *Sl*PatA (Envigo, PA) and with commercially available polyclonal rabbit α-AcK antibodies (Calbiochem). As shown in figure

3, we detected *Sl*PatA in cell lysates when the *S. lividans* wild-type strain was grown in each of the culture media used. As expected, a signal for *Sl*PatA was not detected in the *S. lividans* Δ*patA* strain grown in parallel. Notably, the *Sl*PatA signal was weaker at the 24-h time point than at later time points for all conditions, and *Sl*PatA was not detected at the 62-h time point when the *S. lividans* wild-type strain was grown in media supplemented with β-hydroxybutyrate as the sole carbon source. Similarly, *Sl*PatA was not detected at the 48- and 62-h time points when the *S. lividans patA*$^+$ strain was grown on *N*-acetylglucosamine as the sole carbon source. These data suggested that *Sl*PatA was expressed in a growth-phase dependent manner on each carbon source tested.

Sl*PatA controls acetylation of multiple targets in *S. lividans. When we probed *S. lividans* soluble proteins for AcK residues, we detected differential banding patterns on each carbon source that correlated with the presence of *Sl*PatA (Fig. 3). It is important to note that we observed a high number of proteins acetylated in the absence of *Sl*PatA in all conditions, suggesting that *Sl*PatA-independent acetylation occurs in *S. lividans*. This was not surprising since non-enzymatic acetylation occurs (Weinert *et al.*, 2013, Kuhn *et al.*, 2014), and the genome of *S. lividans* codes for 72 putative acetyltransferases, some of which are likely to acetylate proteins.

We observed differences in protein acetylation that correlated with the presence of *Sl*PatA when *S. lividans* was grown in minimal and rich medium, suggesting that *Sl*PatA controlled the acetylation of multiple targets (Fig. 3). Notably, when *S. lividans* was grown on *N*-acetylglucosamine, differences in acetylation patterns between *S. lividans patA*$^+$ and Δ*patA* strains correlated strongly with the presence of *Sl*PatA after 24 h of growth. Significant differences in acetylation were not detected at 48- and 62-h time points when *Sl*PatA was not detected. The most striking difference in acetylation patterns between the *patA*$^+$ and Δ*patA* strains occurred when *S. lividans* was grown on β-hydroxybutyrate. As seen in figure 3, *Sl*PatA was detected after 24, 38, and 48 h of growth. We observed acetylated proteins between 50 and 75 kDa in the *S. lividans patA*$^+$ strain that were not detected in the *S. lividans* Δ*patA* strain, suggesting that these proteins were acetylated by *Sl*PatA.

Identification of acetylated proteins in *S. lividans* correlated with the presence of *Sl*PatA. To identify possible targets of *Sl*PatA, *S. lividans* wild-type and Δ*patA* strains were grown on β-hydroxybutyrate as before, and soluble proteins were subjected to isoelectric focusing followed by SDS-PAGE. Gels were stained to confirm equal loading (Fig. 4A, B). *S. lividans* wild-type and Δ*patA* protein were then transferred to polyvinylidene fluoride (PVDF) membrane for western blotting. Acetylated proteins were detected using α-AcK antibodies. We detected six distinct AcK spots in lysates of *S. lividans patA*$^{+}$ strain (Fig. 4C, D) that were not found in lysates of a *S. lividans* Δ*patA* strain (Fig. 4E).

Acetylated protein spots were excised from the corresponding isoelectric point and molecular mass position from duplicate, Coomassie Blue-stained protein gels. Proteins of interest were identified by mass spectrometry peptide fingerprinting (spectra not shown). We identified four acid:CoA (AMP-forming) ligases among the six spots detected (Table 1). All of the putative CoA ligases activate organic acids to the corresponding thioester in the two-step reaction shown Fig. 1, 5A. Spots 1 and 2 were fragments of the same protein (EFD65796), and proteins EFD65795 and EFD68037 were found in the same location (spot 3). Spot 6 was identified as CTP synthetase, which does not belong to the AMP-forming family of enzymes. CTP synthetase was not further analyzed.

Table 1. Identification of lysine-acetylated proteins by isoelectric focusing / SDS-PAGE, Western blot analysis and LC/MS/MS

Accession number	**Annotation**	**Acetylated site**	**Spot #**
EFD65795	Acid:CoA ligase	PMTVSG**K^{Ac}**VRKVELRE	3, 5
EFD65796	Acetate:CoA ligase	PKTVSG**K^{Ac}**IRRIELRE	1, 2
EFD68037	Acid:CoA ligase	PKTSVG**K^{Ac}**FDKKVLRR	3
EFD64737	Phenylacetate:CoA ligase	LERSLG**K^{Ac}**IRRVWDQR	4
Additional Acid:CoA ligases identified by bioinformatics analysis			
EFD64524	Putative acid:CoA ligase	PLTAVG**K^{Ac}**VDKAALAR	
EFD64965	Putative acid:CoA ligase	PRNASG**K**ILKRELRD	

EFD66106	Putative acid:CoA ligase	PRTATG**K^{Ac}**LQRYRLLD
EFD67678	Putative acid:CoA ligase	PRAASG**K**ILRRQLRE

The single acetylated lysine detected in each protein was the predicted catalytic lysine located within the so-called A10 motif of acid:CoA ligases (AMP-forming) (Starai & Escalante-Semerena, 2004a, Gulick, 2009) (Fig. 5B, black asterisk), suggesting that acetylation could be a means of regulating the activity of these putative *S. lividans* enzymes.

The acetylated, putative *S. lividans* acid:CoA (AMP-forming) ligases are not modified by *Sl*PatA. Since many bacterial acid:CoA (AMP-forming) ligases are known to be acetylated, we sought to determine whether the newly identified enzymes were substrates of *Sl*PatA as suggested by the results shown in figure 4. Purified proteins were incubated with [1-^{14}C]-acetyl-CoA and *Sl*PatA and transfer of the acetyl moiety onto the proteins was monitored by phosphor imaging. Surprisingly, none of the proteins were acetylated by *Sl*PatA under conditions previously optimized for *Sl*PatA (Tucker & Escalante-Semerena, 2013), compared to a positive control of *Sl*PatA with its *bona fide* substrate *Sl*AacS (Fig. S4). This was despite the fact that these CoA ligases were identified in a *patA*$^{+}$ strain.

We began addressing these unexpected results by testing the possibility that the *S. lividans* PatB (*Sl*PatB) acetyltransferase was in fact responsible for the acetylation of the proteins identified by isoelectric focusing/SDS-PAGE.

We chose to test *Sl*PatB, as it is the only other characterized acetyltransferase in *S. lividans* that also targets acid:CoA ligases (VanDrisse & Escalante-Semerena, 2018).

The difference in domain organization between *Sl*PatA (type II) and *Sl*PatB (type III) is illustrated in figure S1. Because of difficulties keeping *Sl*PatB active in isolation, we used the more stable *Sl*PatB homologue from *Micromonospora aurantiaca*, *Ma*PatB (Xu *et al.*, 2014) in our *in vitro* experiments. Previous work from our laboratory showed that *Ma*PatB is functionally and physiologically equivalent to *Sl*PatB (VanDrisse & Escalante-Semerena, 2018). We prepared reaction mixtures that contained *Ma*PatB plus the identified *S. lividans* putative acid:CoA ligases plus [1-^{14}C]-acetyl-CoA. After a 2-h incubation at 37ºC, proteins

were resolved by SDS-PAGE and label transfer visualized by phosphor imaging as described under *Experimental procedures.* As shown in figure 6, two of the four acid:CoA ligases that were identified from mass spectrometry experiments (EFD65795, EFD68037; shown in boldface type) were acetylated by *Ma*PatB. This acetylation appeared on the putative active-site lysine, a conclusion that we reached because K-to-A variants of the ligases were not acetylated, indicating that the substituted lysine residue was the only acetylatable site.

These data highlighted the fact that *Sl*PatA and *Sl*PatB appear to have different protein substrate specificity since *Sl*PatB acetylated proteins that *Sl*PatA did not.

To explore the possibility that *Ma*PatB could acetylate other AMP-forming acid:CoA ligases in *S. lividans*, the primary amino acid sequence of the acetate:CoA ligase (Acs) from *S. lividans* was used to search for putative acid:CoA ligases in this bacterium using the BLASTp algorithm (Altschul *et al.*, 2009). Four genes encoding putative CoA ligases with sequences with the highest degree of identity to Acs were cloned, overexpressed, and the proteins purified (Table 1). These proteins also contained predicted active-site lysine residues (Fig. 5B), making them putative candidates for acetylation. When these additional proteins were incubated with *Ma*PatB and [1-^{14}C]-
acetyl-CoA, two of the proteins, EFD64524 and EFD66106 (shown in boldface type), were acetylated (Fig. 6). As with other acetylatable proteins, the acetylation was specific to the putative active-site lysine since the EFD64524^{K540A} and EFD66106^{K550A} variants were not acetylated by *Ma*PatB (Fig. 6). Interestingly, the acid:CoA ligases EFD64737, EFD67678, EFD65796, and EFD64965 were not acetylated by *Ma*PatB indicating there might be additional acid:CoA ligase acetyltransferases in *S. lividans* capable of acetylating these CoA ligases.

Acetylated *S. lividans* CoA ligases are deacetylated by NAD$^+$-dependent sirtuin. To determine whether acetylation of *S. lividans* enzymes was reversible, as has been the case for CoA ligases in other organisms (Crosby *et al.*, 2012a, Starai & Escalante-Semerena, 2004b, Gardner *et al.*, 2006, Tucker & Escalante-Semerena, 2013, Burckhardt *et al.*, 2019).

S. lividans CoA ligases were acetylated with [1-^{14}C]-acetyl-CoA and incubated with the known sirtuin deacylase CobB from *S. enterica*. We did not use the sirtuin deacylases from *S. lividans* (*Sl*SrtA, *Sl*CobB) because they are inactive *in vitro* even though they are active *in vivo* (Tucker & Escalante-Semerena, 2013, VanDrisse & Escalante-Semerena, 2018); *Se*CobB is ~30% identical to the sirtuins from *Streptomyces lividans* (Fig. S5). The EFD64524^{Ac} protein was unstable during the deacetylation assay, hence its deacetylation status could not be assessed. While ligases EFD65795^{Ac} and EFD68037^{Ac} were deacetylated by the *Se*CobB sirtuin, EFD66106^{Ac} was not (Fig. 7), a finding that reinforces the idea that it is difficult to predict based solely on sequence which proteins may be substrates for acetyltransferases and deacetylases.

***S. lividans* CoA ligases activate a variety of substrates.** All of the above mentioned acid:CoA ligases were previously uncharacterized and their acid targets unknown. To determine the organic acid substrates for each of the new CoA-ligases, each enzyme was purified and their enzymatic activity was quantified using the continuous spectrophotometric assay described under *Experimental procedures*.

A variety of organic acids were found to be substrates of the CoA ligases (Fig. 8). EFD65795, EFD65796, and EFD64524 activated short chain fatty acids. EFD65795 activated several aliphatic linear, branched, and unsaturated 4- and 5-carbon fatty acids. Thus, we named EFD65795 LbuL for linear, branched, and unsaturated fatty acid:CoA ligase. The specific activity of EFD65796 was the highest when C3 and C4 substrates were used. The enzyme activated isobutyrate ~4-fold faster than propionate and butyrate. EFD65796 was named IbuL for isobutyrate:CoA ligase. The apparent substrate preference for EFD64565 was not as clear since it showed similar specific activities with butyrate, valerate and caproate. However, dicarboxylic fatty acids were not good substrates for this enzyme. Because of the similar specific activities with C4, C5 and C6 monocarboxylates, we refrained from naming EFD64565 until catalytic efficiencies are determined for each substrate. EFD68037 activates 5- to 12-carbon linear fatty acids and was named MlaL for medium and long chain fatty acid:CoA ligase. Other CoA ligases activated aromatic acids.

EFD64737 was annotated as a phenylacetic acid CoA ligase (PaaL) and displayed a preference for this substrate over related aromatic organic acids. EFD66106 specifically activated 2-aminobenzoate and was named AmbL for 2-aminobenozate:CoA ligase. EFD64524 showed homology to 2,3-dihydroxybenozoate:CoA ligases and displayed higher specific activity for that compound, thus we named it DhbL for 2,3-dihydroxybenzoate:CoA ligase. We named EFD67678 as a 4-coumarate:CoA ligase, CouL. Table 2 shows the correspondence between locus tags, functions, and newly assigned protein names based on functionalities. Kinetic parameters must be determined for each enzyme and each substrate to be able to conclude which substrates are likely to be the preferred substrates for each enzyme.

Table 2. Names of *S. lividans* acid:CoA ligases based on substrate range

Locus tag	Substrates	Name	Acetylated by *Ma*PatB
EFD64524	2,3-Dihydroxybenzoate	DhbL	Yes
EFD64795	Isovalerate, valerate, butyrate, crotonate	LbuL	Yes
EFD64796	Isobutyrate, propionate, butyrate	IbuL	No
EFD64737	Phenylacetate	PaaL	No
EFD64965	Valerate, butyrate, caproate	EFD64965	No
EFD66106	2-aminobenzoate	AmbL	Yes
EFD67678	4-coumarate	CouL	No
EFD68037	Caproate, valerate, heptanoate	MlaL	Yes

Activity of CoA ligases is regulated by acetylation. To determine the impact of acetylation on activity, MlaL and LbuL were incubated with *Ma*PatB with or without acetyl-CoA. After incubation, MlaL was tested for CoA ligase activity with caproate and LbuL with isovalerate (Fig. 9). Upon acetylation by *Ma*PatB, activity of each CoA ligase tested decreased only marginally (~20% decrease in the activities of $MlaL^{Ac}$ and $LbuL^{Ac}$).

A buffer sweep for *Ma*PatB activity was performed at pH values ranging from 5 to 9.5. Buffer and pH changes did not appear to make a difference in activity of LbuL after acetylation at pH between 6.5 and 9.5; the protein was unstable below pH 6.5 (data not shown). However, while these changes were modest, the decrease in activity was similar to that seen after *Ma*PatB acetylation of *Sl*Acs (VanDrisse & Escalante-Semerena, 2018, Xu *et*

al., 2014). This idea is discussed further in the *Discussion* section. These data are consistent with known *S. lividans* acetylation systems, indicating regulation of these CoA ligases may occur *in vivo*.

Discussion

The metabolic capabilities of actinobacteria are broad and complex. *S. lividans* is no exception. By studying a few of its putative acid:CoA ligases, we have learned that the substrate specificity of the these enzymes is broad, probably evolving in response to the richness of organic acids present in the soil, where this organism is found. In soil, organic acid concentration can be as high as 1 mM for monocarboxylic acids, and as high as 50 μM for polycarboxylates, providing soil bacteria with a plethora of carbon and energy to be extracted (Adeleke *et al.*, 2017). Among the organic acid substrates activated by just a few of the *S. lividans* CoA ligases, our studies revealed that these enzymes can activate aliphatic linear, saturated and unsaturated, short and medium length and aromatic organic acids (Fig. 8, Table 2). The large number of putative CoA ligases encoded by the genome of this bacterium suggests that these types of compounds are critical carbon and energy sources for *S. lividans*, and likely for other streptomycetes.

Why does *S. lividans* posttranslationally control the activity of some CoA ligases? Although the activity of some, but not all, of its CoA ligases that we studied were under the control of the sirtuin-dependent protein acylation/deacylation systems tested (Figs. 4, 5, 6), it is important to note that the lack of acetylation in some cases could be due to the fact that the acetyltransferase that modifies such enzymes was not used in this work. We note that the *S. lividans* genome encodes >70 putative GNATs (Hentchel & Escalante-Semerena, 2015), hence it would be premature to conclude that CoA ligases that were not acetylated by *Sl*PatA or *Ma*PatB (the homologue of *Sl*PatB) are not under RLA control. These results raise questions, such as i) what are the physiological stresses that trigger the acylation of proteins? ii) which organic acids are used to modify proteins? iii) what acetyltransferase(s) acetylate the other CoA ligases, if any, iv) what are the targets of the other uncharacterized

acetyltransferases in *S. lividans*? etc. Clearly, more work is needed to answers these questions. Regardless, our data provide evidence that reversible lysine acetylation (RLA) occurs in this bacterium, and that it is likely to play an important role in the metabolism and physiology of diverse organic acids.

Insights into the complexity of the role of reversible lysine acetylation in *S. lividans*. One striking result obtained during the course of these studies was that while the results of the initial screen for AcK correlated the presence of *Sl*PatA with the acetylation of four CoA ligases (Fig. 4), none of the identified proteins was a substrate of *Sl*PatA *in vitro.* In fact, only two of the four proteins were acetylated *in vitro*, and the acetyltransferase catalyzing the transfer was not *Sl*PatA. Based on results obtained with *Ma*PatB (a homologue of *Sl*PatB), we speculate that *Sl*PatB may control the activity of the *Ma*PatB-acetylatable CoA ligases (Table 2), but the signals that trigger the modification are unknown. Alternatively, one or more of the yet-to-be-studied putative acetyltransferases may be responsible for the acetylation of the CoA ligases that were not acetylated by *Sl*PatA *in vitro* but their acetylation *in vivo* correlated with the presence of *Sl*PatA. What we do know is that *Sl*PatA synthesis appears to be regulated as a function of the growth phase and the carbon and energy source available to the bacterium (Fig. 3). From a physiological stand point, this observation makes sense, since the CoA ligases studied here are ATP-consuming, AMP-forming enzymes and under nutrient limited conditions, cells must reduce the rate of ATP consumption.

The fact that the absence of *Sl*PatA did not affect the growth of *S. lividans* when different carbon and energy sources were provided suggests that the growth conditions used did not elicit the stress signals needed for the control of any CoA ligases involved in the catabolism of the substrates provided.

Target specificity of *Sl*PatA *vs Sl*PatB. The differential patterns of acetylated proteins that correlate with the presence of *Sl*PatA suggest that many proteins are under the control of this enzyme (Fig. 3). Because the results presented in figure 3 were not confirmed *in vitro* in

experiments performed with purified components, we surmise that *Sl*PatA is indirectly involved in the acetylation of the proteins identified in figure 3, and that the enzyme responsible for the modification of the protein targets is *Sl*PatB or a yet-to-be-identified acetyltransferase. One possible explanation for this observation could be that *Sl*PatA somehow controls *patB* transcription. Control of gene expression by reversible lysine acetylation is not unprecedented in actinobacteria (Ghosh *et al.*, 2016) gamma- and alpha-proteobacteria (Thao *et al.*, 2010, Lima *et al.*, 2011, Christensen *et al.*, 2018), and *Firmicutes* (Carabetta *et al.*, 2019). If in fact *Sl*PatA somehow affects the *patB* transcription, the newly identified *Sl*PatB substrates would not be acetylated in a Δ*patA* strain of *S. lividans.* As mentioned above, it is unclear that *Sl*PatB is the enzyme that modifies the CoA ligases that were acetylated *in vitro.* Additional work linking the catabolism of specific organic acids to *Sl*PatA and *Sl*PatB function is needed to provide *in vivo* support to the *in vitro* data reported herein.

Physiological importance of reversible lysine acetylation of CoA ligases in *S. lividans*. Substrates for the eight putative AMP-forming CoA ligases were identified, expanding the known metabolic capabilities of *Streptomyces*. Four of these CoA ligases (LbuL, IbuL, MlaL, and PaaL) are acetylated during growth on β-hydoxybutyrate as compared to growth on rich or minimal glucose (Fig. 4). This could indicate an increased need to regulate these enzymes under the conditions tested. Three of the CoA ligases enriched for acetylation (LbuL, IbuL, and MlaL) activate short to medium length organic acids, while PaaL activates phenylacetate (Fig. 8). Phenylacetyl-CoA is converted in several steps into acetyl-CoA and succinyl-CoA before entering central metabolism. β-Hydoxybutyrate is metabolized into acetoacetate, which can be converted into acetoacetyl-CoA, which in turn can be converted into AcCoA to generate energy and building blocks (Pauli & Overath, 1972). We note here, that the activation of acetoacetate into acetoacetyl-CoA by *Sl*PatA is under RLA control (Tucker & Escalante-Semerena, 2013). This fact raises the possibility of multiple layers of RLA control taking place simultaneously in *S. lividans.* But, why are these ligases posttrranslationally controlled in *S. lividans?* There is precedent in the literature that shows

that RLA control of the AMP-forming acetate:CoA ligase Acs of *S. enterica* maintains the energy charge of the cell (Chan *et al.*, 2011). That is, lack of RLA control of Acs leads to growth arrest because of Acs-dependent depletion of ATP and the concomitant rise in AMP, resulting in an energy charge that cannot support cell growth (Chan *et al.*, 2011). By inactivating an AMP-forming acetate:CoA ligase, the cell can modulate the amount of AMP produced. It is plausible that *S. lividans* acetylates CoA ligases for the purpose of maintaining energy charge homeostasis while growing on organic acids.

Why does the modification of the catalytic lysine of CoA ligases have a limited effect on enzyme activity? When assaying the impact of acetylation by *Ma*PatB, activity of MlaL and LbuL reproducibly decreased ~20% (Fig. 9). However, while these changes were modest, the decrease in activity was similar to that seen after *Ma*PatB acetylation of *Sl*Acs (VanDrisse & Escalante-Semerena, 2018, Xu *et al.*, 2014). As was the case for *Sl*Acs, the limited decrease in enzymatic activity in acetylated CoA ligases may be linked to the degree of acetylation of a serine residue within the acetylation motif (Fig. 5B, yellow highlight), which in the case of *Sl*Acs was needed for lysine acetylation by *Sl*PatB (VanDrisse & Escalante-Semerena, 2018). This serine modification only occurred *in vivo* in *S. lividans* and it is possible that these CoA ligases would need to be purified from *S. lividans* and tested for their acetylation ability by *Sl*PatB. The alluded acetylated serine may be needed for recognition and acetylation of the CoA ligases. Ongoing work is aimed at elucidating the role of serine acetylation in the regulation of CoA ligase activity in *S. lividans*.

Alternative explanations for our results. One area of interest that remains mostly unexplored is how the activity of GNATs is controlled. To date, evidence of allostery has been reported for type III GNATs (Xu *et al.*, 2014), but not for type I or II. It is possible that some of the proteins identified *in vivo* as substrates for *Sl*PatA were not acetylated *in vitro* by *Sl*PatA because an effector or accessory protein was absent in the reaction mixture. These possibilities will be explored in future studies.

A wealth of information is yet to be uncovered. As mentioned above, the *S. lividans* genome encodes ~72 putative GNATs, a fact that reflects on the diversity of stimuli that likely cause metabolic stress in this bacterium. At present, there is limited information about the function of these enzymes and the signals that control their activities. While studies of the function and regulation of such putative enzymes is a tall order, the insights that such efforts would provide valuable information regarding the physiology of actinobacteria.

Experimental procedures

Bacterial strains and growth conditions. All strains and plasmids used in this study are listed in Table 3. *Streptomyces* strains are derivatives of *Streptomyces lividans* TK24. ISP-2 medium (Shirling & Gottlieb, 1966) or R2YE medium (Kieser *et al.*, 2000b) was used to culture *S. lividans* on solid medium. Liquid cultures of *S. lividans* were inoculated with 1 x 10^9 spores (Kieser *et al.*, 2000a).

Table 3. Strains and plasmids used in this study[1].

Name	Relevant Genotype	Reference or source
E. coli strains		
JE9314	Strain C41(DE3) *pka12*::*kan*$^+$	Laboratory collection
S. lividans strains		
TK24	Wild type	Laboratory collection
Derivatives of *S. lividans* TK24		
JE16707	Δ*patA*	
Plasmids		
pMHT238Δ	Encodes the etch tobacco virus (TEV) protease with a truncation of its last four residues, and a His_7 tagged fused on its *N*-terminus	(Blommel & Fox, 2007)
pTEV5	Over expression vector, *bla*$^+$. Genes cloned into this vector encode proteins with a *N*-terminal, rTEV-cleavable His_6-tag	(Rocco *et al.*, 2008)
Derivatives of plasmid pTEV5		
p*Sl*MlaL1	*S. lividans mlaL*$^+$ (formerly EFD68037)	
p*Sl*MlaL2	*S. lividans mlaL1* (encodes variant $MlaL^{K538A}$)	
p*Sl*LbuL1	*S. lividans lbuL*$^+$ (formerly EFD65795)	

p*Sl*LbuL2	*S. lividans lbuL1* (encodes variant LbuL^{K527A})	
p*Sl*AmbL1	*S. lividans ambL*$^{+}$ (formerly EFD66106)	
*pSl*AmbL2	*S. lividans ambL1* (encodes variant EFD66106^{K550A})	
p*Sl*CouL1	*S. lividans couL*$^{+}$ (formerly EFD67678)	
p*Sl*CouL2	*S. lividans couL1* (encodes variant EFD67678^{K512A})	
p*Sl*EFD64965-1	*S. lividans EFD64965*$^{+}$	
p*Sl*EFD64965-2	*S. lividans* p*Sl*EFD64965-2 (encodes variant EFD64965^{K492A})	
p*Sl*DhbL1	*S. lividans dhbL*$^{+}$ (formerly EFD64524)	
*pSl*DhbL2	*S. lividans dhbL1* (encodes variant EFD64524^{K538A})	
p*Sl*PaaL1	*S. lividans paaL*$^{+}$ (formerly EFD64737)	
p*Sl*PaaL2	*S. lividans paaL1* (encodes variant PaaA^{K540A})	
p*Sl*IbuL1	*S. lividans ibuL*$^{+}$ (formerly EFD65796)	
p*Sl*IbaL2	*S. lividans ibuL1* (encodes variant IbuL^{K534A})	

[1]Unless otherwise stated, all strains and plasmids were constructed during the course of this work.

S. lividans was grown in yeast extract-malt extract (YEME) rich medium (Kieser *et al.*, 2000b). *S. lividans* liquid cultures were grown in baffled flasks with marine-grade stainless steel springs to aid in cell dispersion. Strains were cultured for 72 h at 30°C.

Unless noted otherwise, all *E. coli* strains used were derivatives of *E. coli* C41 (DE3). *E. coli* strains were grown at room temperature or 37°C in lysogeny broth (LB, Difco) (Bertani, 1951). When necessary ampicillin was used at 100 μg ml^{-1}.

Preparation of *S. lividans* cell-free extracts. Twenty or 25 ml of *S. lividans* cultures was diluted into 25 ml of distilled water. Cells were harvested by centrifugation for 10 min at 4,000 x *g*. Cell pellets were washed once with 25 ml of *tris*-(hydroxymethyl)aminomethane-HCl (Tris-HCl, pH 7.5 @ 25°C) buffer and excess buffer was removed by decantation. Cell pellets were weighed and flash frozen in liquid nitrogen.

Cells were stored at -80°C until lysis. *S. lividans* cells were resuspended in 0.5 or 1 ml lysis buffer [4-(2-hydroxyethyl)-1-piperazineethanesulfonic acid (HEPES, 50 mM), NaCl (100 mM), lysozyme (1 mg ml^{-1}), DNase (50 μg ml^{-1}), SIGMAFAST Protease Inhibitor Cocktail Tablet (EDTA-free, 0.01 tablet ml^{-1}), and phenylmethanesulfonylfluoride (PMSF, 0.5 mM). Cells were placed on ice and lysed by sonication for 2 s (0.2-s pulse followed by 0.2- s

cooling). Samples were centrifuged at 40,000 x *g* for 30 min to remove insoluble material. Soluble proteins were quantified using the Bio-Rad Protein assay according to the manufacturer's protocol (Bio-Rad).

One-dimensional Western blot analysis. For one-dimensional gel analysis fifty micrograms of cellular protein were resolved using SDS-PAGE (Laemmli, 1970) and transferred onto a PVDF membrane (Millipore). Rabbit polyclonal *Sl*PatA antiserum (Laboratory Animal Resources, University of Wisconsin, Madison, WI) was used to detect *Sl*PatA (1:10,000 final dilution). Rabbit polyclonal α-AcK antibodies were used to detect acetylated proteins (Calbiochem, 1:5,000 dilution). Binding of primary antibodies to blots was visualized using alkaline phosphatase-conjugated goat α-rabbit immunoglobulin G (ThermoFisher) and NBT/BCIP 1-Step substrate (Pierce) according to the manufacturer's instructions.

Two-dimensional Western blot analysis. Two-dimensional electrophoresis was performed according to the carrier ampholine method of isoelectric focusing (Talmi-Frank *et al.*, 2009, O'Farrell, 1975) by Kendrick Labs, Inc. (Madison, WI). Duplicate gels were run for lysates of *S. lividans* TK24 and *S. lividans* Δ*patA* strains grown on NMMP supplemented with β-hydroxybutyrate (10 mM) for 60 h. Isoelectric focusing was performed in a glass tube of 3.3-mm inner diameter using 2.0% pH 4-8 mix Servalytes (Serva, Heidelberg, Germany; and 2 mM lysine) for 20,000 V-h. One μg of an IEF internal standard, tropomyosin, was added to each sample. This protein migrated as a doublet with lower polypeptide spot of MM 33,000 Da and pI 5.2. The enclosed tube gel pH gradient plot for this set of Servalytes was determined with a surface pH electrode.

After equilibration for 10 min in Buffer O (10% (v/v) glycerol, dithiothreitol (DTT, 50 mM), SDS (2.3% w/v) and Tris-HCl buffer (0.0625 M, pH 6.8), each tube gel was sealed to the top of a stacking gel that overlaid a 10% (w/v) acrylamide slab gel (1.00 mm thick). SDS slab gel electrophoresis was performed for about 5 h at 25 mA/gel. The following proteins (Sigma Chemical Co., St. Louis, MO) were used as molecular mass standards (Da): myosin

(220,000), phosphorylase A (94,000), catalase (60,000), actin (43,000) carbonic anhydrase (29,000) and lysozyme (14,000). These standards appear as bands at the basic edge of the Coomassie Brilliant Blue R-250-stained gel. The gel was dried between sheets of cellophane with the acid edge to the left.

After slab gel electrophoresis, the gels for blotting were placed in transfer buffer *N*-cyclohexyl-3-aminopropanesulfonic acid (CAPS, 10 mM, pH 11.0, 10% (v/v) MeOH) and transblotted onto a PVDF membrane overnight at 225 mA and approximately 100 V/ two gels. Membranes were de-stained with 10% (v/v) methanol prior to blotting. Acetylated lysine residues were detected as described above. Corresponding spots were cut from the duplicate gels, and samples were analyzed by mass spectrometry.

*Determination of the acetylated proteins by mass spectrometry***.** To determine the identity of the acetylated proteins identified by 2-D gel electrophoresis, "In Gel" digestion and mass spectrometric analysis was performed at the Proteomics and Mass Spectrometry Facility (University of Georgia). Mass spectrometry analyses were performed using a Thermo-Fisher LTQ Orbitrap Elite Mass Spectrometer coupled with a Proxeon Easy NanoLC system (Waltham, MA). Peptides were loaded into a Dionex PepMap 5 mm long and 300-μm internal diameter pre-column (Sunnyvale, CA) first, then were separated by a self-packed ~12-cm long, 100-μm internal diameter column/emitter with 200 Å 5 μM Burker MagicAQ C18 (Auburn, CA), at 500 μL by gradient elution. Briefly, the two-buffer gradient (0.1% (v/v) formic acid as buffer A and
99.9% acetonitrile with 0.1% formic acid(v/v) as buffer B) starts with 5% B, increases to 40% B in 40 min, to 60% B in 15 min, and to 95% B in 10 min. The Top 10 data-dependent acquisition method was used to acquire data. Both MS and MS/MS scans were analyzed using Orbitrap at the resolutions of 120,000 and 30,000, respectively. Proteome Discoverer 1.3 (Thermo- Fisher) software was used with Mascot database search program (Matrix Science, Landon, UK) for protein
identifications.

Plasmid construction. All primers used in this study were synthesized by IDT (Coralville, IA) and are listed in table 4.

Table 4. List of primers used in this study

Primer	Sequence
EFD65795 5' NheI pTEV5	GTAGCTAGCATGACCGCACCCGCGCCCCAGC
EFD65795 3' EcoRI pTEV5	ACTGAATTCTCAGGGGCGCGTTCCGTACCGC
EFD65796 5' NheI pTEV5	GTAGCTAGCATGACGACGGCCACGGAGCTG
EFD65796 3' EcoRI pTEV5	ACTGAATTCTCACCGGAAGTCCTCCTCGCGG
EFD68037 5' NheI pTEV5	GTAGCTAGCATGTCGCCCCGGGAGGACAC
EFD68037 3' EcoRI pTEV5	ACTGAATTCTCAGAGCCGGGTGACGTCGAG
EFD64737 NheI pTEV5	GTAGCTAGCATGAGCAGCGAGCCGACGAC
EFD64737 EcoRI pTEV5	ACTGAATTCTCACGCGCCCCGCTGGTC
EFD66106 5' NheI pTEV5	GTAGCTAGCATGTCGTCACCAACACGATACGCTCG
EFD66106 3' EcoRI pTEV5	ACTGAATTCTTATGTCGTCGGCGTCGCGC
EFD67678 5' NheI pTEV5	GTAGCTAGCATGTTCCGCAGCGAGTACGC
EFD67678 3' EcoRI pTEV5	ACTGAATTCTCATCGCGGCTCCCTGAGC
EFD64965 5' NheI pTEV5	GTAGCTAGCATGACGCCCGGACACGGCAGC
EFD64965 3' EcoRI pTEV5	ACTGAATTCTCAGGCACCGGCGAAGCGGTCC
EFD64524 5' NheI pTEV5	GTAGCTAGCATGAGCAAGACTCAACGGACC
EFD64524 3' EcoRI pTEV5	ACTGAATTCTCACGGCCGGGGCAACTGC
EFD65795 5' K527A	CACCTTGCGCACCGCCCCCGAGACGGTC
EFD65795 3' K527A	GACCGTCTCGGGGGCGGTGCGCAAGGTG
EFD68037 5' K538A	CACCTTCTTGTCGAACGCGCCGACGCTCGTCTTC
EFD68037 3' K538A	GAAGACGAGCGTCGGCGCGTTCGACAAGAAGGTG
EFD64737 5' K438A	CACCCGGCGGATCGCGCCGAGCGAGCGC
EFD64737 3' K438A	GCGCTCGCTCGGCGCGATCCGCCGGGTG
EFD65796 5' K534A	GATGCGGCGGATCGCGCCCGAGACGGTC
EFD65796 3' K534A	GACCGTCTCGGGCGCGATCCGCCGCATC
EFD64524 5' K540A	CGCCTTGTCGACCGCCCCGACCGCGGTG
EFD64524 3' K540A	ACCGCGGTCGGGGCGGTCGACAAGGCG
EFD64965 5' K492A	CCCTCTTGAGGATCGCCCCGCTGGCGTTGC
EFD64965 3' K492A	GCAACGCCAGCGGGGCGATCCTCAAGAGGG
EFD67678 5' K512A	CGGCGGAGGATCGCGCCGGAGGCGGC
EFD67678 3' K512A	GCCGCCTCCGGCGCGATCCTCCGCCG
EFD66106 5' K550A	GTAGCGCTGGAGCGCGCCGGTCGCCGTG
EFD66106 3' K550A	CACGGCGACCGGCGCGCTCCAGCGCTAC

All primers

were synthesized by IDT (Coralville, IA)

Streptomyces lividans TK24 genomic DNA was used as template to amplify genes *lbuL* (EFD65795), *ibuL* (EFD65796), *mlaL* (EFD68037), *paaL* (EFD64737), *dhbL* (EFD64524), *EFD64965*, *couL* (EFD67678), and *ambL* (EFD66106) genes for overproduction using Pfu Ultra II Fusion DNA polymerase (Agilent). The first codon of *lbuL* (GTG) was changed to the more common ATG start codon. The DNA fragments were digested with NheI and EcoRI and ligated into pTEV5 that directs the synthesis of the recombinant protein fused to a hexa-his (H_6) tag at the *N*-terminus (Rocco *et al.*, 2008). Site-directed mutagenesis for constructing active-site lysine variants was performed using the QuikChange protocol (Stratagene) using the plasmid containing the wild-type allele as template. DNA sequencing of resulting plasmids was performed at the Georgia Genomics and Bioinformatics Core at the University of Georgia.

Overproduction of proteins. Overproduction plasmids were transformed into a derivative of *E. coli* strain C41(λDE3) Δ*pka* (*pka* codes for the acid:CoA ligase acetyltransferase of *E. coli)* to block acetylation during overproduction. Cells carrying overproduction plasmids were grown at 37°C for ~ 4 h and then diluted 1:50 (v/v) into 2 L of LB containing ampicilin (100 μg ml^{-1}) and grown at room temperature (~25°C) with shaking at 150 rpm. Gene expression was induced when cultures reached an optical density at 600 nm (Spectronic 20D) of 0.3-0.4. At that point, IPTG (500 μM) was added to the culture, which was grown overnight at room temperature with shaking in an *innova®44* (New Brunswick Scientific) gyratory shaker. Cells were harvested by centrifugation at 6,000 x *g* for 15 min at 4°C in an Avanti J-2 XPI centrifuge equipped with rotor JLA- 8.1000 (Beckman Coulter), and the cell paste was frozen at -80°C until use.

Purification of *S. lividans* CoA ligase proteins. Frozen cell pellets were resuspened in 30-40 ml cold bind buffer containing 4-(2-hydroxyethyl)-1-piperazineethanesulfonic acid (HEPES) buffer (50 mM, pH 7.5 @ 4 ºC) containing NaCl (500 mM) and imidazole (20 mM), lysozyme (1 μg ml^{-1}), DNase (25 μg ml^{-1}), and phenylmethanoesulfonyl fluoride (PMSF,

Fisher Scientific; 0.5 mM). Cells were lysed by sonication (550 Sonic Dismembrator, Fisher Scientific) at an amplitude setting of 60 for 2 s on, followed by 2 s off for 30 s on ice for four cycles total. Cellular debris was cleared by centrifugation at 40,000 x *g* for 30 min in an Avanti J-25I floor centrifuge equipped with a JA-25.25 rotor (Beckman Coulter).

Clarified cell-free extract was loaded onto a 1-ml Ni-NTA affinity column (HisPur; ThermoFisher Scientific) equilibrated with bind buffer. The column was washed with 10 column volumes of bind buffer to remove unbound proteins followed by six column volumes of wash buffer containing HEPES buffer (50 mM, pH 7.5 @ 4 ºC) containing NaCl (500 mM) and imidazole (60 mM). Proteins were eluted with six column volumes of elution buffer containing HEPES buffer (50 mM, pH 7.5 @ 4 ºC) containing NaCl (500 mM) and imidazole (500 mM).

Fractions containing the desired H_6-tagged proteins were pooled and rTEV protease was added (1:50 mg/mg ratio) and incubated at room temperature for 3 h to allow for cleavage of the H_6 tag. This mixture was dialyzed at 4ºC against a HEPES buffer (50 mM, pH 7.5 @ 4 ºC) containing NaCl (500 mM) three times for at least three h each. The cleaved and dialyzed protein was passed over the 1-ml Ni-NTA equilibrated with bind buffer and washed as described above. Cleaved protein passed through the resin and eluted in the flow-through fractions while un-cleaved protein remains bound to the resin. Fractions were analyzed by SDS-PAGE, and those containing the desired protein were pooled and dialyzed at 4ºC against a HEPES buffer (50 mM, pH 7.5 @ 4 ºC) containing NaCl (150 mM) and 10% (v/v) glycerol before storage at -80ºC.

Purification of *M. aurantiaca* PatB acetyltransferase protein. *Ma*PatB was purified as described above but in a Tris-HCl buffer (50 mM, pH 7.5 @ 4 ºC) containing NaCl (500 mM) and 20% (v/v) glycerol and various levels of imidazole. For cleavage of the H_6 *N*-terimal tag, rTEV protease was added at a 1:10 mg/mg ratio and incubated as described above since uncleaved H_6-*Ma*PatB was inactive (data not shown). De-tagged protein was loaded onto 1-ml Ni-NTA column equilibrated with Tris-HCl buffer (50 mM, pH 7.5 @ 4 ºC) containing NaCl

(500 mM), 0.5mM TCEP, and 20% (v/v) glycerol. Fractions of the flow through containing cleaved *Ma*PatB were pooled and used for assays.

***In vitro* acetylation and deacetylation assays**. Assays were performed as described (Burckhardt *et al.*, 2019). Briefly, reactions containing HEPES buffer (50 mM, pH 7 @ 24ºC), *tris*(2-carboxyethyl)phosphine (TCEP, 1 mM), [1-^{14}C]-AcCoA (40 μM; spec. rad. = 57.1mCi/mmol), *Ma*PatB (3 μM), and CoA ligase (3 μM) or lysine variant of a CoA ligase (3 μM) were incubated at 37ºC for 2 h to transfer the radiolabeled acetyl group to a target protein. Reactions were quenched with loading dye (60% (v/v) glycerol, Tris-HCl pH 6.8 (0.3 M), EDTA (12 mM), 12% SDS, 2-mercaptoethanol (0.87 mM), bromophenol blue (0.05%, w/v) and reaction mixtures were resolved by SDS-PAGE on a 12% (w/v) polyacrylamide gel with Tris-HCl buffer pH 8.8 (resolving gel)/Tris-HCl pH 6.8 (stacking gel). The SDS-PAGE gel was stained using Coomassie Brillant Blue R (MPBiomedicals), and radioactivity distribution was visualized using a phosphor imager after 24-36 h of exposure. A Typhoon Trio+ Variable Mode Imager (GE Health Life Sciences) with ImageQuant v5.2 software was used to quantify the intensity of signals. Optimal assay conditions for *Sl*PatA were reported previously (Tucker & Escalante-Semerena, 2013).

For deacetylation assays, LbuL (EFD65795), MlaL (EFD68037), and AmbI (EFD66106) were first acetylated using *Ma*PatB as described above. Reaction mixtures containing LbuL and MlaL were buffer exchanged using Amicon® Ultra Centrifugal Filters (Millipore; 3,000 NMWL) to remove un-incorporated [1-^{14}C]-AcCoA while reaction mixtures containing AmbL (EDF66106) were not buffer exchanged because AmbL fell out of solution during buffer exchange. Instead, 1 mM CoA was added to outcompete un-incorporated [1-^{14}C]-AcCoA in reactions containing AmbL. The sirtuin *Se*CobB (3 μM) was added to acetylated CoA ligases (3 μM) and incubated at 37ºC for 2 h. NAD^+ (1 mM). Samples from deacetylation reaction mixtures resolved by SDS-PAGE on a 12% (w/v) polyacrylamide gel and radioactivity distribution was determined as described above. Deacetylation assays were performed with $DhbL^{Ac}$ ($EFD64524^{Ac}$), but the protein was unstable and its deacetylation status could not be assessed.

***In* vitro acyl-CoA ligases activity assays.** Activity of *S. lividans* CoA ligases was measured using a continuous spectrometric assay (Crosby *et al.*, 2012a, Burckhardt *et al.*, 2019). Reactions mixtures (100 μL) contained HEPES buffer (50 mM, pH 7 @ 24ºC), TCEP (1 mM), ATP (2.5 mM), CoA (0.5 mM), $MgCl_2$ (5 mM), KCl (1 mM), phosphoenolpyruvate (3 mM), NADH (0.1 mM), pyruvate kinase (1 U), myokinase (5 U), lactate dehydrogenase (1.5 U), and purified CoA ligase (10- 300 nM). Reactions were started by the addition of either acetate, propionate, butyrate, valerate, caproate, heptanoate octanoate, nonanoate, decanoate, undecanoate, laurate, tridecanoate, myristate, oxalate, malonate, succinate, glutarate, adipate, pimelate, suberate, azelate, sebacate, undecanedioate, dodecanedioate, fumarate, acetoacetate, hydroxybutyrate, butyrate, isovalerate, crotonate, isobutyrate, methylmalonate, benzoate, methylsuccinate, 3-(methylthio)propionate, 3-phenylpropionate, 4-phenylbutyrate, 2-phenylpropionate, 2-aminobenozoate, 3-aminobenzoate, and 4-aminobenzoate (0.2 mM) or 2,3-dihydroxybenzoate, 2,4-dihydroxybenzoate, 3,4-dihydroxybenzoate, and 3,5-dihydroxybenzoate (2 mM). NADH-consumption was measured at 340 nm every 5 s over an 8-min time span at 30ºC using a SpectraMax Plus 384 microplate spectrophotometer (Molecular Devices). Enzyme activities were calculated as described (Garrity *et al.*, 2007) and graphed using Prism v6 (GraphPad) software. Specific activity data are presented with standard deviations from duplicate experiments performed in technical triplicate.

Acknowledgements

The authors declare no conflict of interest. Data are available upon request from the authors. This work was supported by NIH grant R35-GM130399 to J.C.E.-S. Peptide fingerprinting was performed at the Proteomics and Mass Spectrometry Facility of the University of Georgia.

Data availability. Data sharing not applicable.

References

Adeleke, R., Nwangburuka, C., and Oboirien, B. (2017) Origin, roles and fate of organic acids in soils: a review. *S. Afr. J. Bot.* **108**: 393.

Altschul, S.F., Gertz, E.M., Agarwala, R., Schaffer, A.A., and Yu, Y.K. (2009) PSI-BLAST pseudocounts and the minimum description length principle. *Nucleic Acids Res.* **37**: 815-824.

Bertani, G. (1951) Studies on lysogenesis. I. The mode of phage liberation by lysogenic *Escherichia coli*. *J. Bacteriol.* **62**: 293-300.

Blommel, P.G., and Fox, B.G. (2007) A combined approach to improving large-scale production of tobacco etch virus protease. *Protein Expr. Purif.* **55**: 53-68.

Burckhardt, R.M., Buckner, B.A., and Escalante-Semerena, J.C. (2019) *Staphylococcus aureus* modulates the activity of acetyl-Coenzyme A synthetase (Acs) by sirtuin-dependent reversible lysine acetylation. *Mol. Microbiol.* **112**: 588-604.

Carabetta, V.J., Greco, T.M., Cristea, I.M., and Dubnau, D. (2019) YfmK is an N(epsilon)-lysine acetyltransferase that directly acetylates the histone-like protein HBsu in *Bacillus subtilis*. *Proc. Natl. Acad. Sci. U S A* **116**: 3752-3757.

Chan, C.H., Garrity, J., Crosby, H.A., and Escalante-Semerena, J.C. (2011) In *Salmonella enterica*, the sirtuin-dependent protein acylation/deacylation system (SDPADS) maintains energy homeostasis during growth on low concentrations of acetate. *Mol. Microbiol.* **80**: 168-183.

Christensen, D.G., Meyer, J.G., Baumgartner, J.T., D'Souza, A.K., Nelson, W.C., Payne, S.H., Kuhn, M.L., Schilling, B., and Wolfe, A.J. (2018) Identification of novel protein lysine acetyltransferases in *Escherichia coli*. *MBio* **9**: e01905-18

Crosby, H.A., and Escalante-Semerena, J.C. (2014) The acetylation motif in AMP-forming acyl coenzyme A synthetases contains residues critical for acetylation and recognition by the protein acetyltransferase Pat of *Rhodopseudomonas palustris*. *J. Bacteriol.* **196**: 1496-1504.

Crosby, H.A., Pelletier, D.A., Hurst, G.B., and Escalante-Semerena, J.C. (2012a) System-wide studies of *N*-lysine acetylation in *Rhodopseudomonas palustris* reveal substrate specificity of protein acetyltransferases. *J. Biol. Chem.* **287**: 15590-15601.

Crosby, H.A., Rank, K.C., Rayment, I., and Escalante-Semerena, J.C. (2012b) Structural insights into the substrate specificity of the protein acetyltransferase *Rp*Pat: Identification of a loop critical for recognition by *Rp*Pat. *J. Biol. Chem.* **287**: 41392-41404.

Frey, P.A., and Arabshahi, A. (1995) Standard free energy change for the hydrolysis of the alpha, beta-phosphoanhydride bridge in ATP. *Biochemistry* **34**: 11307-11310.

Gardner, J.G., and Escalante-Semerena, J.C. (2009) In *Bacillus subtilis*, the sirtuin protein deacetylase encoded by the *srtN* gene (formerly *yhdZ*), and functions encoded by the *acuABC* genes control the activity of acetyl-CoA synthetase. *J. Bacteriol.* **191**: 1749-1755.

Gardner, J.G., Grundy, F.J., Henkin, T.M., and Escalante-Semerena, J.C. (2006) Control of acetyl-coenzyme A synthetase (AcsA) activity by acetylation/deacetylation without NAD^+ involvement in *Bacillus subtilis*. *J. Bacteriol.* **188**: 5460-5468.

Garrity, J., Gardner, J.G., Hawse, W., Wolberger, C., and Escalante-Semerena, J.C. (2007) *N*-lysine propionylation controls the activity of propionyl-CoA synthetase. *J. Biol. Chem.* **282**: 30239-30245.

Ghosh, S., Padmanabhan, B., Anand, C., and Nagaraja, V. (2016) Lysine acetylation of the *Mycobacterium tuberculosis* HU protein modulates its DNA binding and genome organization. *Mol. Microbiol.* **100**: 577-588.

Gulick, A.M. (2009) Conformational dynamics in the acyl-CoA synthetases, adenylation domains of non-ribosomal peptide synthetases, and firefly luciferase. *ACS Chem. Biol.* **4**: 811-827.

Gulick, A.M., Starai, V.J., Horswill, A.R., Homick, K.M., and Escalante-Semerena, J.C. (2003) The 1.75Å crystal structure of acetyl-CoA synthetase bound to adenosine-5'-propylphosphate and coenzyme A. *Biochemistry* **42**: 2866-2873.

Hallows, W.C., Lee, S., and Denu, J.M. (2006) Sirtuins deacetylate and activate mammalian acetyl-CoA synthetases. *Proc. Natl. Acad. Sci. U S A* **103**: 10230-10235.

Hentchel, K.L., and Escalante-Semerena, J.C. (2015) Acylation of biomolecules in prokaryotes: a widespread strategy for the control of biological function and metabolic stress. *Microbiol. Mol. Biol. Rev.* **79**: 321-346.

Kieser, T., Bibb, M.J., Buttner, M.J., Chater, K., and Hopwood, D.A., (2000a) Growth and preservation of *Streptomyces*. In: Practical *Streptomyces* Genetics. Norwich, England: John Innes Foundation, pp. 43-62.

Kieser, T., Bibb, M.J., Buttner, M.J., Chater, K., and Hopwood, D.A., (2000b) Media, buffers, and suppliers. In: Practical *Streptomyces* Genetics. Norwich, England: John Innes Foundation, pp. 405-420.

Kuhn, M.L., Zemaitaitis, B., Hu, L.I., Sahu, A., Sorensen, D., Minasov, G., Lima, B.P., Scholle, M., Mrksich, M., Anderson, W.F., Gibson, B.W., Schilling, B., and Wolfe, A.J. (2014) Structural, kinetic and proteomic characterization of acetyl phosphate-dependent bacterial protein acetylation. *PLOS ONE* **9**: e94816.

Laemmli, U.K. (1970) Cleavage of structural proteins during the assembly of the head of bacteriophage T4. *Nature* **227**: 680-685.

Lima, B.P., Antelmann, H., Gronau, K., Chi, B.K., Becher, D., Brinsmade, S.R., and Wolfe, A.J. (2011) Involvement of protein acetylation in glucose-induced transcription of a stress-responsive promoter. *Mol. Microbiol.* **81**: 1190-1204.

Nambi, S., Gupta, K., Bhattacharya, M., Ramakrishnan, P., Ravikumar, V., Siddiqui, N., Thomas, A.T., and Visweswariah, S.S. (2013) Cyclic AMP-dependent protein lysine acylation in mycobacteria regulates fatty acid and propionate metabolism. *J. Biol. Chem.* **288**.

O'Farrell, P.H. (1975) High resolution two-dimensional electrophoresis of proteins. *J. Biol. Chem.* **250**: 4007-4021.

Pauli, G., and Overath, P. (1972) *ato* Operon: a highly inducible system for acetoacetate and butyrate degradation in *Escherichia coli*. *Eur. J. Biochem.* **29**: 553-562.

Reger, A.S., Carney, J.M., and Gulick, A.M. (2007) Biochemical and crystallographic analysis of substrate binding and conformational changes in acetyl-CoA synthetase. *Biochemistry* **46**: 6536-6546.

Robert, X., and Gouet, P. (2014) Deciphering key features in protein structures with the new ENDscript server. *Nucleic Acids Res.* **42**: W320-324.

Rocco, C.J., Dennison, K.L., Klenchin, V.A., Rayment, I., and Escalante-Semerena, J.C. (2008) Construction and use of new cloning vectors for the rapid isolation of recombinant proteins from *Escherichia coli*. *Plasmid* **59**: 231-237.

Shirling, E.B., and Gottlieb, D. (1966) Methods for characterization of *Streptomyces* species. *Int. J. Syst. Bacteriol.* **16**: 313-340.

Starai, V.J., Celic, I., Cole, R.N., Boeke, J.D., and Escalante-Semerena, J.C. (2002) Sir2-dependent activation of acetyl-CoA synthetase by deacetylation of active lysine. *Science* **298**: 2390-2392.

Starai, V.J., and Escalante-Semerena, J.C. (2004a) Acetyl-coenzyme A synthetase (AMP forming). *Cell. Mol. Life Sci.* **61**: 2020-2030.

Starai, V.J., and Escalante-Semerena, J.C. (2004b) Identification of the protein acetyltransferase (Pat) enzyme that acetylates acetyl-CoA synthetase in *Salmonella enterica*. *J. Mol. Biol.* **340**: 1005-1012.

Talmi-Frank, D., Jaffe, C.L., and Baneth, G. (2009) Quantitative computerized western blotting. *Methods Mol. Biol.* **536**: 103-113.

Thao, S., Chen, C.S., Zhu, H., and Escalante-Semerena, J.C. (2010) N(epsilon)-Lysine acetylation of a bacterial transcription factor inhibits its DNA-binding activity. *PLOS ONE* **5**: e15123.

Thauer, R.K., Jungermann, K., and Decker, K. (1977) Energy conservation in chemotrophic anaerobic bacteria. *Bacteriol. Rev.* **41**: 100-180.

Tsang, A.W., and Escalante-Semerena, J.C. (1998) CobB, a new member of the SIR2 family of eucaryotic regulatory proteins, is required to compensate for the lack of nicotinate mononucleotide:5,6-dimethylbenzimidazole phosphoribosyltransferase activity in cobT mutants during cobalamin biosynthesis in *Salmonella typhimurium* LT2. *J. Biol. Chem.* **273**: 31788-31794.

Tucker, A.C., and Escalante-Semerena, J.C. (2013) Acetoacetyl-CoA synthetase activity is controlled by a protein acetyltransferase with unique domain organization in *Streptomyces lividans*. *Mol. Microbiol.* **87**: 152-167.

VanDrisse, C.M., and Escalante-Semerena, J.C. (2018) In *Streptomyces lividans*, acetyl-CoA synthetase activity is controlled by *O*-serine and *N*(varepsilon)-lysine acetylation. *Mol. Microbiol.* **107**: 577-594.

VanDrisse, C.M., and Escalante-Semerena, J.C. (2019) Protein Acetylation in Bacteria. *Annu. Rev. Microbiol.* **73:** 111-132.

Vetting, M.W., Carvalho, L.P.S.d., Yu, M., Hegde, S.S., Magnet, S., Roderick, S.L., and Blanchard, J.S. (2005) Structure and functions of the GNAT superfamily of acetyltransferases. *Arch. Biochem. Biophys.* **433**: 212-226.

Weinert, B.T., Iesmantavicius, V., Wagner, S.A., Scholz, C., Gummesson, B., Beli, P., Nystrom, T., and Choudhary, C. (2013) Acetyl-phosphate is a critical determinant of lysine acetylation in *E. coli*. *Mol. Cell* **51**: 265-272.

Xu, J.Y., You, D., Leng, P.Q., and Ye, B.C. (2014) Allosteric regulation of a protein acetyltransferase in *Micromonospora aurantiaca* by the amino acids cysteine and arginine. *J. Biol. Chem.* **289**: 27034-27045.

Figure legends

Figure 1. Two-step conversion of acetate into acetyl-CoA by AMP-forming acetate:CoA ligase (Acs). A. The first half of the reaction yields acetyl-AMP plus pyrophosphate and in the second half of the reaction CoA displaces AMP, yielding acetyl-CoA. The first half reaction is unfavorable ($\Delta G^{o'}$ = 10.04 kJ mol^{-1}), but the hydrolysis of pyrophosphate ($\Delta G^{o'}$ = -21.92 kJ mol^{-1}) helps drive the reaction forward. B. The second half of the reaction is also favorable ($\Delta G^{o'}$ = -55.65 kJ mol^{-1}) (Thauer *et al.*, 1977, Frey & Arabshahi, 1995). Each half reaction is catalyzed by Acs in a different conformation (Gulick *et al.*, 2003, Reger *et al.*, 2007).

Figure 2. Reversible protein acetylation in bacteria. Gcn5-related acetyltransferases (a.k.a. GNATs) modify the epsilon amino group (*N*ε) of lysine side chains effecting a change in the biological function of the protein target. In some cases, the modification is reversed by different classes of deacetylases. Some of the latter belong to class III deacetylases that are structural homologues to the eukaryotic Sir2 protein, hence the name sirtuin. Sirtuins use NAD^+ as co-substrate and yield *O*-acetyl-ADP-ribose (*O*-AADPR) and nicotinamide (Nm). Zn-dependent, acetate-forming deacetylases belonging to the histone deacetylases are homologous to the AcuC protein of *B. subtilis* (Gardner & Escalante-Semerena, 2009).

Figure 3. Acetylation profiles correlate with PatA in *S. lividans*. *S. lividans* lysates from cells grown on rich medium (YEME) or minimal medium containing Glucose (10 mM), β-hydroxybutyrate (10 mM), or *N*-acetylglucosamine (10 mM) were resolved by SDS-PAGE in triplicate gels (as described in figure S2). One gel was stained with Coomassie Blue to visualize proteins. The remaining two gels for each condition were transferred to PVDF membranes and probed with rabbit polyclonal antibodies against *Sl*PatA (α-*Sl*PatA) or against acetyllysine (α-AcK). Binding of the primary antibodies was visualized using secondary antibodies conjugated to alkaline phosphatase and NBT/BCIP detection. *, molecular mass (kDa).

Figure 4. Resolution of soluble proteins from cell-free extracts of *S. lividans patA*$^+$ and Δ*patA* strains. Two-dimensional gel electrophoresis was used to resolve the soluble proteins of wild-type (A) and Δ*patA* (B) strains of *S. lividans*. Equal total proteins were loaded for both strains for each isoelectric focusing strip (first dimension, pH 4-8). Two technical replicates were run. Shown here is one replicate from each sample stained with Coomassie Brilliant Blue R. The second replicate for each protein sample was transferred to a PVDF membrane for Western blot. MMM, molecular mass markers (kDa). Identical gels to those in panels A and B were transferred to PVDF membranes for Western blot analysis and probed with α-AcK antibodies to detect proteins containing AcK [panel C (*patA*$^+$), and panel E (Δ*patA*)]; prominent AcK-containing proteins in the *patA*$^+$ strain are shown in the inset in

panel D. Proteins represented by each number: 1. EFD65796, 2: EFD65796, 3: EFD68037, EFD65795 4: EFD64737, 5: EFD35795. Degradation of proteins EFD65796 (spots 1, 2) and protein EFD65795 was detected by mass spectrometry. Notably, proteins EFD68037 and EFD65795 had very similar isoelectric points (5.2 and 5.4, respectively) and mass (60362 and 59124 Da, respectively), explaining why both were detected in spot 3. Spot 6 was identified as CTP synthetase.

Figure 5. AMP-forming CoA ligases. A. Two-step CoA ligase reaction. B. Protein alignment of putative CoA ligases from *S. lividans* with known acetyl-CoA synthetase Acs. The conserved active site lysine is marked by a black asterisk. Protein sequences were aligned using Geneious software (www.geneious.com) and the figure was generated using ESPript (Robert & Gouet, 2014). Red highlights indicate conserved residues and boxed residues indicate similar residues.

Figure 6. Acetylation of CoA ligases by the type-III GNAT *Ma*PatB. Purified CoA ligases and lysine variants were incubated with [1-^{14}C]-AcCoA with or without *Ma*PatB. Reactions were resolved on an SDS-PAGE gel and label distribution was visualized by phosphor imaging. Top panel shows the SDS-PAGE and the bottom panel shows the phosphor image of the above gel. MMM (kDa), refers to molecular mass markers, expressed in kilo-Daltons. A positive control of *Sl*Acs and *Ma*PatB was included in each gel, as this acetylation event has been previously characterized (VanDrisse & Escalante-Semerena, 2018).

Figure 7. *Streptomyces* CoA ligases are deacetylated by the *S. enterica* CobB sirtuin deacylase. CoA ligases were acetylated with [1-^{14}C]-AcCoA and incubated with *Se*CobB with or without NAD^+ (1 mM) to remove the radiolabel. Reactions were resolved on an SDS-PAGE gel and label distribution was visualized by phosphor imaging. Top panel shows the SDS-PAGE and the bottom panel shows the phosphor image of the gel.

Figure 8. Characterization of new AMP-forming CoA ligases. Purified CoA ligases were tested with a variety of organic acids and activity was measured using an NADH consumption assay (see *Experimental procedures*). Data represent mean ± S.D. of duplicate experiments done in technical triplicate.

Figure 9. Acetylation of CoA ligases impacts enzyme activity. CoA ligases MlaL (A) and LbuL (B) were incubated with *Ma*PatB with or without acetyl-CoA (AcCoA). After incubation, CoA ligase activity was determined for acetylated and unacetylated proteins using a CoA ligase activity assay (see *Experimental procedures*) with caproate used for MlaL and isovalerate used for LbuL. Data represent mean ± SEM (standard error of the mean) of duplicate experiments.

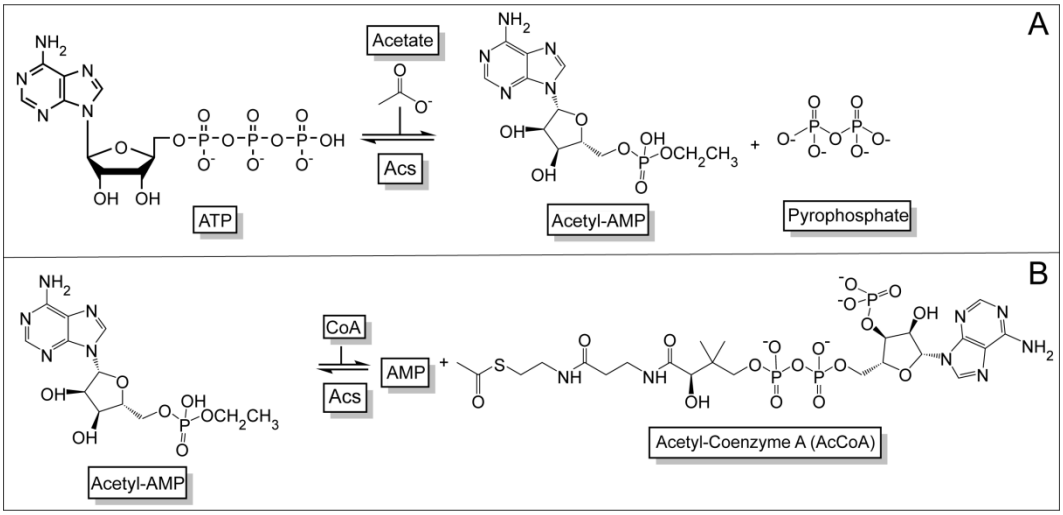

mmi_14414_f1.tif

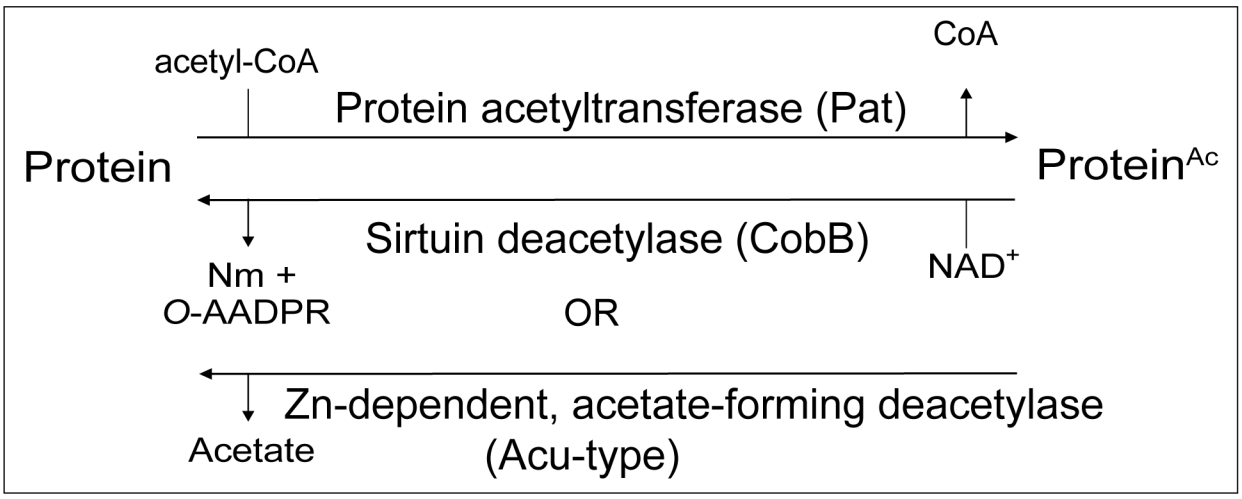

mmi_14414_f2.tif

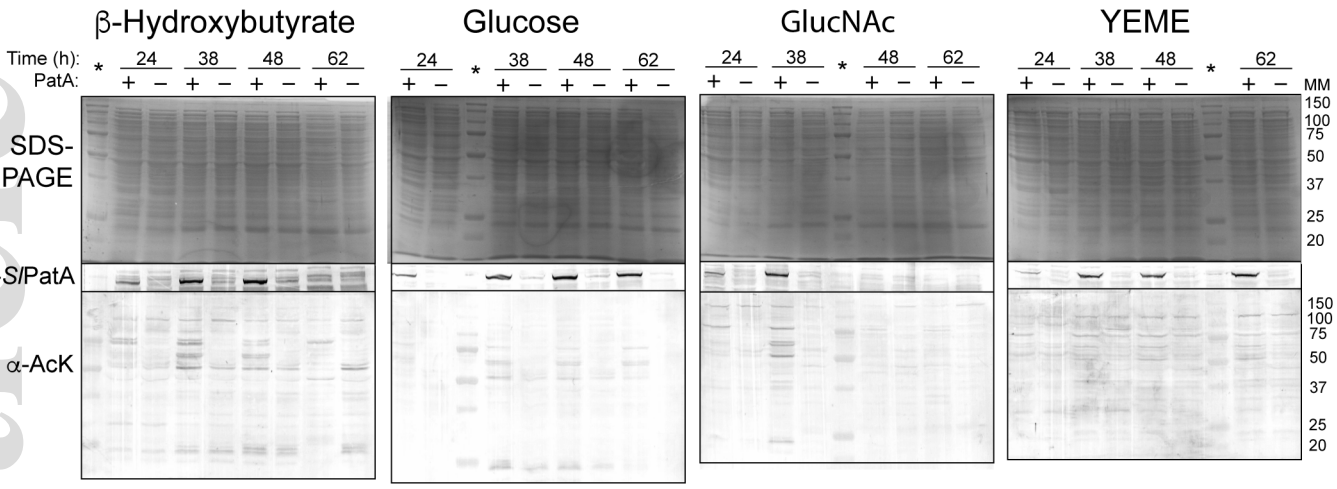

mmi_14414_f3.tif

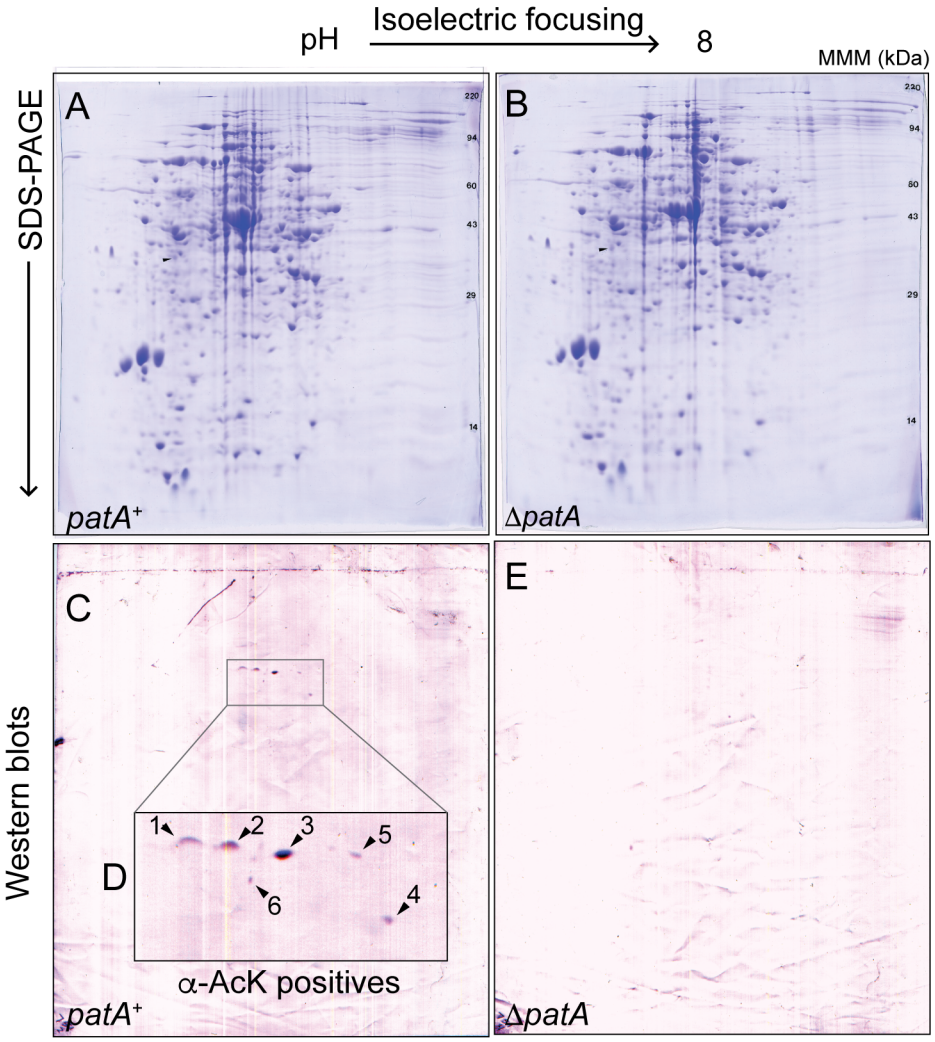

mmi_14414_f4.tif

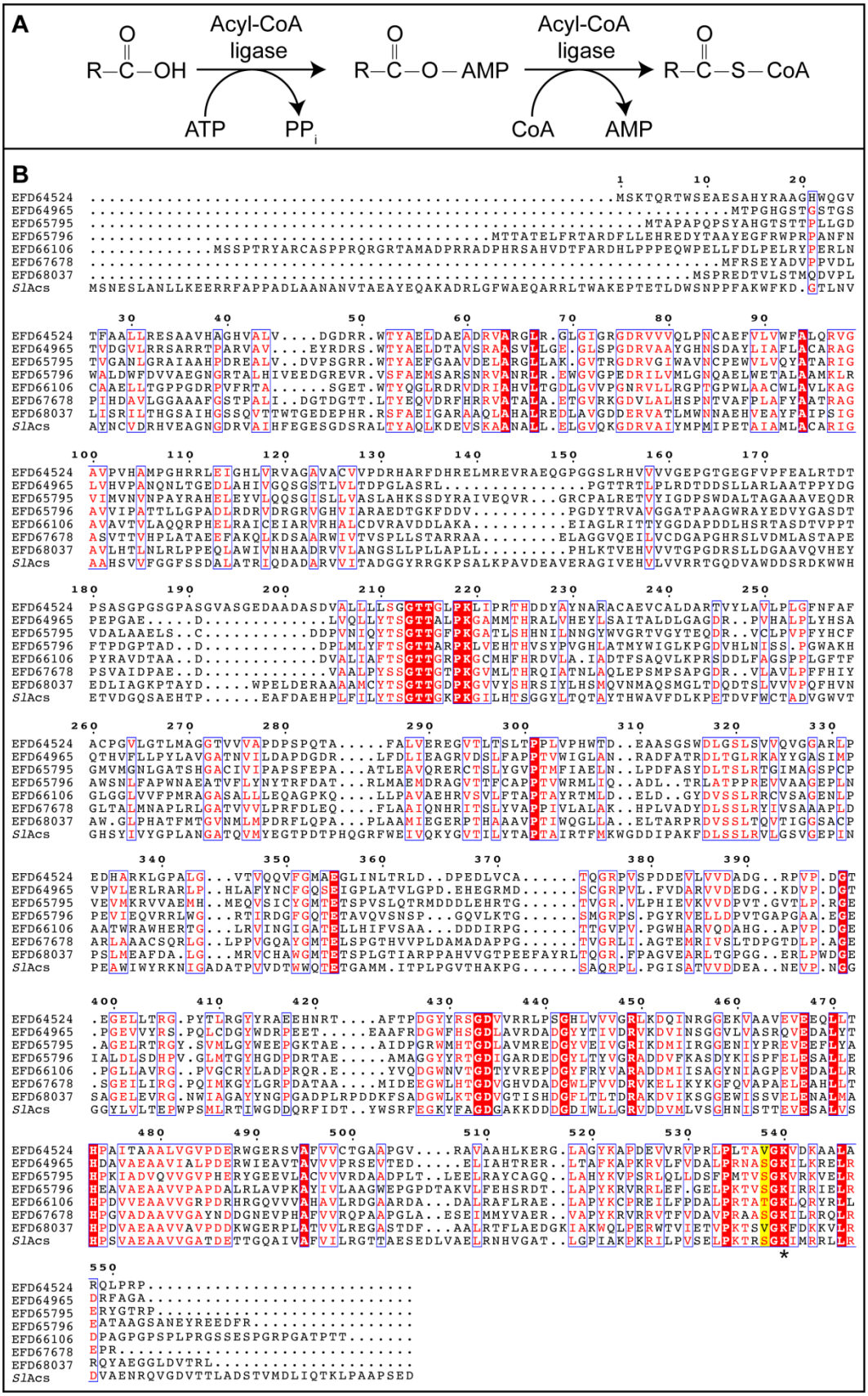

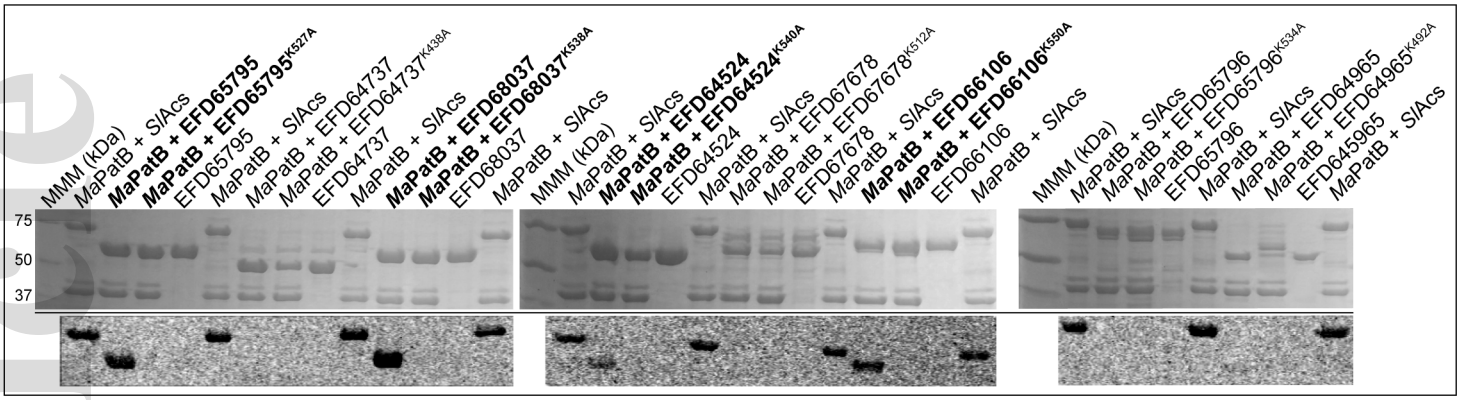

mmi_14414_f6.tif

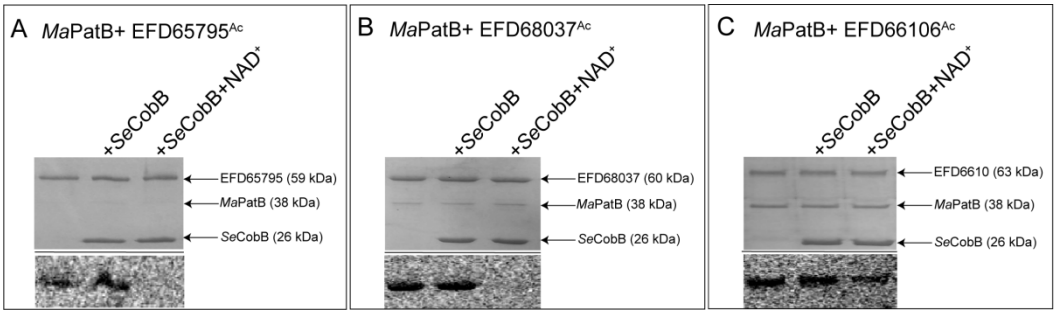

mmi_14414_f7.tif